RSC Advances

RSC Publishing

PAPER

Synthesis, structure and DNA binding studies of 9-phenyldibenzo[*a*,*c*] phenazin-9-ium†

Cite this: *RSC Advances*, 2013, **3**, 3054

Suman Kundu,[a] Manas Kumar Biswas,[a] Ananya Banerjee,[b] Kakali Bhadra,[cd] Gopinatha Suresh Kumar,[c] Michael G. B. Drew,[e] Ranjan Bhadra[a] and Prasanta Ghosh*[a]

Received 27th September 2012,
Accepted 20th December 2012

DOI: 10.1039/c2ra22317a

www.rsc.org/advances

The reaction of phenanthrene-9,10-dione with *N*-phenylbenzene-1,2-diamine in methanol in the presence of anhydrous $CuCl_2$ and HCl affords a 9-phenyldibenzo[*a*,*c*]phenazin-9-ium cation, $[\mathbf{1}]^+$, as in $[\mathbf{1}][CuCl_2]$, in good yields. The reaction of $[\mathbf{1}][CuCl_2]$ in methanol with excess iodide salt affords [**1**][I]. The formations of $[\mathbf{1}][CuCl_2]$ and [**1**][I] have been confirmed by elemental analyses, mass, IR, UV-vis and ^1H NMR spectra including the single crystal X-ray structure determination of $[\mathbf{1}][CuCl_2]$. DNA binding studies by UV-vis spectra, fluorescence spectra, circular dichroism spectra, hydrodynamic, isothermal titration calorimetric (ITC), UV optical melting and gel electrophoresis experiments have substantiated that $[\mathbf{1}]^+$, like ethidium bromide, is a strong DNA intercalator.

Introduction

Small planar heteroaromatic cations are useful and important intercalators with DNA (deoxyribonucleic acid). Strategically, such intercalation prevents information retrieval from DNA, leading to the arrest of cell division including abnormal cell proliferation in cancer.[1] The relevance and importance of this kind of organic[2] and inorganic complex[3] molecules intensified extensive research in drug discovery, including cancer chemotherapy. The syntheses of nitrogen containing planar heteroaromatic cations have been stressed specifically and studies on the intercalation with DNA and small molecules have been conducted over the last five decades in order to indicate not only DNA directed cancer chemotherapy but also diagnostically probe the DNA structure.[2,4] Ethidium bromide, a poly condensate benzophenanthridine (3,8-di-amide substituted), has been well documented as a DNA intercalator and used as a probe to identify new intercalators by displacement studies[5] (Chart 1). In this context, we have been persuaded to isolate new DNA intercalators. In this work, a 9-phenyldibenzo[*a*,*c*]phenazin-9-ium cation, $[\mathbf{1}]^+$, as shown in Chart 1, as the $[\mathbf{1}][CuCl_2]$ salt has been successfully isolated using cupric ions as an oxidizing agent.

The reaction of $[\mathbf{1}][CuCl_2]$ with excess iodide salt affords [**1**][I]. The molecular geometry of $[\mathbf{1}]^+$ has been authenticated by the single crystal X-ray structure determination of $[\mathbf{1}][CuCl_2]$. In this article, UV-vis absorption spectra, an ethidium bromide displacement reaction, circular dichroism, viscosity, gel electrophoresis, hydrodynamic, isothermal titration calorimetric and UV optical melting studies with $[\mathbf{1}][CuCl_2]$ elucidate the structure and behaviour of the $[\mathbf{1}]^+$ cation, which is a strong DNA intercalator.

Experimental section

Materials and physical measurements

Reagents or analytical grade materials were obtained from Sigma-Aldrich Corporation and used without further purification. Spectroscopic grade solvents were used for spectroscopic measurements. The C, H, N contents of the compounds were

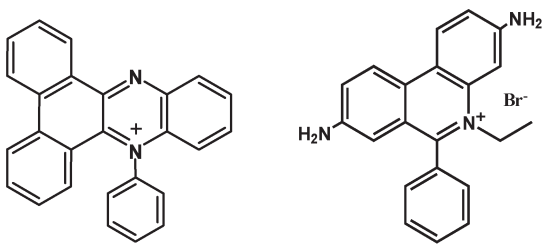

Chart 1 9-Phenyldibenzo[*a*,*c*]phenazin-9-ium $[\mathbf{1}]^+$ and ethidium bromide.

[a]*Department of Chemistry, R. K. Mission Residential College, Narendrapur, Kolkata 700 103, India. E-mail: ghosh@pghosh.in; Fax: +91-33 2477 3597; Tel: +91-33 2428 7347*
[b]*VJRC R&D Center, Vijaygarh Jyotish Ray College, Bijoygarh, Kolkata-700 032, India*
[c]*CSIR-Indian Institute of Chemical Biology, Kolkata 700 032, India*
[d]*Department of Zoology, Kalyani University, Kalyani, West Bengal 741 235, India*
[e]*School of Chemistry, The University of Reading, P.O. Box 224, Whiteknights, Reading, RG6 6AD, UK*

† Electronic supplementary information (ESI) available: Full crystallographic tables (CCDC reference number 893850) of $[\mathbf{1}][CuCl_2]$. For crystallographic data in CIF or other electronic format, see DOI: 10.1039/c2ra22317a

obtained from a *Perkin-Elmer 2400 series II* elemental analyzer. Infrared spectra of the samples were measured from 4000 to 400 cm^{-1} as KBr pellets at room temperature on a *Perkin-Elmer FT-IR-Spectrophotometer Spectrum RX1*. ^1H NMR spectral measurements were carried out on a *Bruker DPX-300 MHz* spectrometer with tetramethylsilane (TMS) as an internal reference. ESI mass spectra were recorded on a micro mass *Q-TOF mass* spectrometer. Electronic absorption spectra in solution at 25 °C were measured on a *Perkin-Elmer Lambda 25* spectrophotometer in the range 200–1100 nm. Fluorescence quenching studies were recorded on a *Perkin-Elmer LS 55* fluorescence spectrophotometer. A *Cannon-Manning semi micro size 75 capillary* viscometer (Cannon Instrument Company, State College, PA, USA) was used for measuring the viscosity. Circular dichroism (CD) spectra were recorded on a *Jasco J 815 spectropolarimeter* (Jasco International Co., Hachioji, Japan) interfaced to a PC and equipped with a thermoelectrically controlled cell holder in rectangular quartz cuvettes of 1 cm path length. The temperature was controlled by a Jasco temperature controller. Isothermal titration calorimetric (ITC) experiments were performed at 20 °C using a *MicroCal VP-ITC* unit (MicroCal Inc.; Northampton, MA, USA). Thermal melting curves of DNA–drug complexes were measured on a *Shimadzu Pharmaspec uv-1700* unit equipped with a Peltier-controlled TMSPC-8 model accessory (Shimadzu Corporation, Kyoto, Japan). Gel documentation was performed by a *BIO-RAD Gel Electrophoresis and Documentation System* (BIO-RAD Pacific Ltd., Hong Kong). *Origin 7.0* software (Origin Lab. Corporation, Northampton, MA, USA) was used for data acquisition and analysis.

Syntheses

[1][CuCl$_2$]. To phenanthrene-9,10-dione (100 mg, 0.5 mmol) in hot methanol (30 mL), *N*-phenylbenzene-1,2-diamine (90 mg, 0.5 mmol) and two drops of concentrated HCl were added successively and the reaction mixture was refluxed for 30 min (at 65 °C). The solution mixture was cooled at room temperature and filtered. To this solution, anhydrous $CuCl_2$ (70 mg, 0.5 mmol) in methanol (10 mL) was added carefully and the reaction mixture was allowed to evaporate slowly at room temperature (25 °C). After a few days, dark coloured crystals of [**1**][$CuCl_2$] separated out, which were collected upon filtration and dried in air. Yield: 225 mg (~90% with respect to copper). Single crystals for X-ray structure determination were picked up from this crop. ESI (positive ion)-MS in CH_3CN; *m*/*z*: 357.84 ([**1**][$CuCl_2$] − $CuCl_2$)$^+$. Anal. calcd for $C_{26}H_{17}Cl_2CuN_2$: C, 63.49; H, 3.48; N, 5.70; found: C, 63.45; H, 3.44; N, 5.65. ^1H NMR (DMSO-d_6, 300 MHz, 22 °C) δ (ppm) = 9.45 (d, 1H), 8.78 (d, 1H), 8.67 (d, 1H), 8.56 (d, 1H), 8.27 (t, 1H), 8.19 (t, 1H), 7.92 (m, 8H), 7.75 (q, 1H), 7.57 (t, 2H). IR (KBr, ν_{max}/cm^{-1}): = 3424(m), 3041(m), 1602(s), 1448(m), 1362(vs), 1271(s), 1155(s), 1105(vs), 755(vs), 716(s), 704(s), 579(s).

[1][I]. To [**1**][$CuCl_2$] (100 mg, 0.2 mmol), methanol (50 mL) was added, stirred (~45 min) and filtered. To the filtrate methanolic solution (10 mL), KI (200 mg, 1.2 mmol) was added and the reaction mixture was stirred for 1 h at room temperature (25 °C). A white precipitate of CuI separated out. The mixture was filtered and the filtrate was allowed to evaporate slowly at room temperature. After a few days, a black crystalline solid separated out, which was collected upon filtration. The crystalline residue of [**1**][I] was dried in air. Yield: 80 mg (~80%). ESI (positive ion)-MS in CH_3CN; *m*/*z*: 357.84 ([**1**]$^+$). Anal. calcd for $C_{26}H_{17}IN_2$: C, 64.48; H, 3.54; N, 5.78; found: C, 64.05; H, 3.34; N, 5.62. ^1H NMR (DMSO-d_6, 300 MHz, 22 °C) δ (ppm) = 9.45 (d, 1H), 8.78 (d, 1H), 8.67 (d, 1H), 8.56 (d, 1H), 8.27 (t, 1H), 8.19 (t, 1H), 7.92 (m, 8H), 7.75 (q, 1H), 7.57(t, 2H). IR (KBr, ν_{max}/cm^{-1}): = 3428(m), 3017(m), 2362(m), 1601(s), 1448(m), 1445(m), 1365(vs), 1272(s), 1156(s), 1106(vs), 761(vs), 717(s), 708(m), 581(m).

X-ray crystallographic data collection and refinement of [1][CuCl$_2$]

A dark brown shining crystal of [**1**][$CuCl_2$] was picked up with a nylon loop and was mounted on an *Oxford Diffraction X-Calibur System* equipped with a graphite monochromator (Mo-Kα, λ = 0.71073 Å). Final cell constants were obtained from the least squares fits of all measured reflections. The intensities of the data were corrected for absorption using the intensities of redundant reflections. The structures were readily solved by direct methods and subsequent difference Fourier techniques. The crystallographic data are listed in Table 1. A *ShelXTL97*[6] software package was used for solution of the structure. *ShelXL97*[6] was used for the refinement. All non-hydrogen atoms were refined anisotropically. Hydrogen atoms were placed at the calculated positions and refined as riding atoms with isotropic displacement parameters.

DNA binding studies

Calf thymus DNA (CT-DNA, type I, 42% GC content) and analytical grade ethidium bromide (EB) [3,8-di-amino-5-ethyl-6-phenylphenanthridium] were used without further purification. The buffer used throughout the study was prepared as 10 mM potassium phosphate (KP buffer), pH 7.0 ± 0.2, with 50 mM NaCl. After dissolving the salts in deionised double distilled water they were sterilised in a microwave oven (heating 2 min) and filtered with a 0.45 μm pore size membrane to remove any particulate matter. Both CT-DNA and EB were made into a solution in the fresh buffer and the concentration was determined by taking the molar extinction

Table 1 Crystallographic data of [**1**][$CuCl_2$]

Formula	$C_{26}H_{17}Cl_2CuN_2$	*T*/K	150(2)
F_W	491.86	ρ_c/g cm^{-3}	1.558
Crystal colour	Black	Uniq. reflections	10605
Crystal system	Monoclinic	Reflections	5655
Space group	$P2_1/n$	$2\theta_{max}$	58.60
a/Å	7.5536(4)	*F*(*000*)	1000
b/Å	18.6217(6)	R_1[a] [$I > 2\sigma(I)$]	0.0322
c/Å	14.9419(13)	R_1[a] (all data)	0.0606
β/?	93.727(6)	GoF[b]	0.856
V/Å^3	2097.3(2)	wR_2[c] [$I > 2\sigma(I)$]	0.0789
Z	4	Param./restr.	280/0
λ/Å / μ/mm^{-1}	0.71073/1.313	Residual density/eÅ^{-3}	0.420/-0.329

Observation criterion: $I > 2\sigma(I)$. [a] $R1 = \Sigma||F_o| - |F_c||/\Sigma|F_o|$. [b] GoF = $\{\Sigma[w(F_o^2 - F_c^2)2]/(n - p)\}^{1/2}$. [c] $wR2 = \{\Sigma[w(F_o^2 - F_c^2)_2]/\Sigma[w(F_o^2)_2]\}^{1/2}$. Where $w = 1/[\sigma^2(F_o^2) + (aP)^2 + bP]$, $P = (F_o^2 + 2F_c^2)/3$.

coefficient (ε_0); 6600 M^{-1} cm^{-1} and 5680 M^{-1} cm^{-1} for CT-DNA and EB, respectively. The ratio of absorption of the CT-DNA solution at 260/280 nm was about 1.8, indicating that the CT-DNA was free from contaminating protein. The absorption maxima (λ_{max}) of CT-DNA and EB were considered to be 260 nm and 480 nm, respectively, to estimate the concentration of their solutions using their respective molar extinction coefficients (ε_0).

The planar heteroaromatic complex [**1**][$CuCl_2$] was soluble in dimethyl sulfoxide (DMSO) and its concentration was determined spectrophotometrically, taking its absorption maximum (λ_{max}) and molar extinction coefficient (ε_0) as 440 nm and 21 600 M^{-1} cm^{-1}, respectively. The DMSO dissolved [**1**][$CuCl_2$] solution was serially diluted to an appropriate concentration so that when it was added to a 1 cm path length cuvette there was a total reaction volume of 2.5 mL and the DMSO content was less than 7.5% (v/v). Under these conditions, the planar organic cation $[\mathbf{1}]^+$ was stable and interacted efficiently with DNA. Preliminary spectroscopic binding experiments with [**1**][I] are similar to [**1**][$CuCl_2$] and lead us to study with the more soluble [**1**][$CuCl_2$].

UV-vis spectroscopy

The absorption spectral measurements were done in matching quartz cuvettes of 1 cm path length. A constant amount of DNA (15.2 μM) was placed in the buffer, both in the sample and reference cuvettes maintained at 20 °C, and then titrated with an increasing concentration of [**1**][$CuCl_2$] solution with constant stirring. Briefly, on each addition of the aliquot of [**1**][$CuCl_2$] solution to the DNA and allowing an equilibrium time of about 5 min, the absorbance was recorded. The isosbestic point at 465 nm for [**1**][$CuCl_2$] was determined and the concentration of the total bound [**1**][$CuCl_2$] was calculated (Fig. 1). The absorbances at the isosbestic point (465 nm) (λ_{iso}) and the maximum wavelength (λ_{max}) of the complex [**1**][$CuCl_2$] were determined after each addition. The extinction coefficient of [**1**][$CuCl_2$] at the isosbestic point (ε_{iso}) was determined and the extinction coefficient of bound [**1**][$CuCl_2$] (ε_B) was obtained by addition of a known quantity of [**1**][$CuCl_2$] to a large excess of DNA, corresponding to the saturation point: (ε_B) = λ_{max}/lC_t where l is the path length and C_t is the total [**1**][$CuCl_2$] concentration present, which was calculated as (C_t) = $\lambda_{iso}/\varepsilon_{iso}$. The values of λ_{max}, λ_{iso}, ε_{iso}, and ε_B were determined and these are used to calculate the expected absorbance at the wavelength maxima, $\lambda_{exp} = lC_t\varepsilon_{max}$, where ε_{max} is the molar extinction coefficient at the wavelength maxima. The difference in λ_{exp} and the observed absorbance was used to calculate the amount of bound [**1**][$CuCl_2$]. Then the concentrations of the free (C_f), bound (C_b) and total (C_t) amounts of [**1**][$CuCl_2$] were determined.[7]

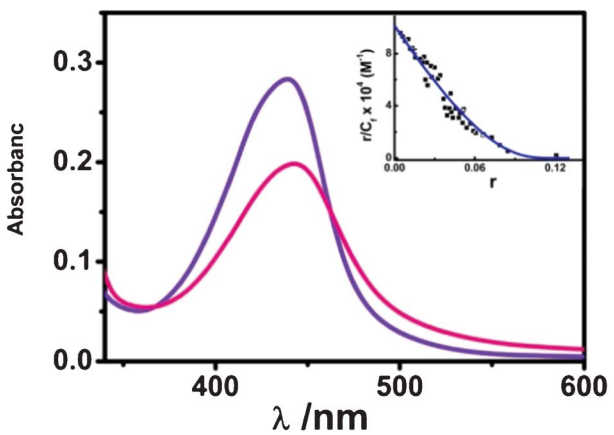

Fig. 1 Plot of absorbance against wavelength showing the spectra of [**1**][$CuCl_2$] (violet) and CT-DNA bound [**1**][$CuCl_2$] (pink). The inset shows the Scatchard plot of the binding.

The binding data were used to construct Scatchard plots of r/C_f *vs.* r, where r is the number of moles of [**1**][$CuCl_2$] bound per mole of DNA base pairs and C_f is the molar concentration of free [**1**][$CuCl_2$]. The binding isotherms were analysed according to the excluded site model of McGhee and von Hippel for a nonlinear, non-cooperative ligand binding system using the equation:[8]

$$\frac{r}{C_f} = K_i(1-nr)\left[\frac{(1-nr)}{\{1-(n-1)r\}}\right]^{(n-1)}$$

where K_i is the intrinsic binding constant to an isolated site and n is the number of base pairs excluded by the binding of a single [**1**][$CuCl_2$] molecule. The binding data were analysed using Origin software to determine the best fit parameters of K_i and n.[9]

Fluorescence emission spectral study

A 1 cm path length quartz cuvette was filled with buffer up to 2.5 mL volume and examined for fluorescence emission after the inclusion of ethidium bromide (EB) or [**1**][$CuCl_2$] or DNA. No emission spectra were observed with any of these alone, but the addition of EB (10.02 μM) to CT-DNA (7.95 μM) and excitation at 525 nm yielded a strong emission spectrum in the range 600–650 nm. The cation [**1**][$CuCl_2$] concentration to quench the fluorescence of the EB–CT-DNA complex more than 50% was determined by titration.

Circular dichroism spectroscopy

Circular dichroism (CD) spectral measurements of CT-DNA and CT-DNA–[**1**][$CuCl_2$] cation complexes were performed in rectangular stain free quartz cuvettes of 1 cm path length at 20 ± 1 °C. The spectra were signal averaged over at least four scans. The scans were accumulated and automatically averaged with scan rate 50 nm min^{-1}, band width 1.0 nm and sensitivity 100 m deg. The molar elipticity values [θ] were calculated from the equation [θ] = $\theta_{obs}/10cl$, where c is the concentration of DNA/$[\mathbf{1}]^+$ and l is the path length of the cuvette. The molar elipticity [θ] (deg cm^2 $dmol^{-1}$) values are expressed in terms of base pairs in the region 200–400 nm or per bound [**1**][$CuCl_2$] in the range 300–500 nm.

Hydrodynamic studies

The viscosity of the DNA–[**1**][$CuCl_2$] complex was estimated by measuring the time of flow in a viscometer mounted vertically in a constant temperature bath maintained at 20 ± 1 °C. The flow times of DNA alone (sonicated to 2–2.5 × 10^5 Daltons) and with different ratios of [**1**][$CuCl_2$] were measured in triplicate by an electronic stopwatch with an accuracy of ±

0.01 s. Viscosity experiments were carried out with ~350 μM CT-DNA. The flow times $t_{control}$, $t_{complex}$ and t_0 were determined for CT-DNA, the CT-DNA–[**1**][$CuCl_2$] complex and the buffer alone by averaging six readings for each. The relative viscosity of various sets was calculated from the relation, $\eta'_{sp}/\eta_{sp} = \{(t_{complex} - t_0)/t_0\}/\{(t_{control} - t_0)/t_0\}$, where η'_{sp} and η_{sp} are the specific viscosity of the CT-DNA–[**1**][$CuCl_2$] complex and CT-DNA alone, respectively.[10]

Gel electrophoresis

The interaction between [**1**][$CuCl_2$] and [**1**][I], stated as drugs, with DNA (250 ng), was studied by agarose gel electrophoresis. Here, pUC19 DNA isolated from *E. coli* DH5α by an alkaline lysis method was incubated with various concentrations of the drugs [**1**][$CuCl_2$] (2.56, 1.92, 1.28 and 0.64 mM) and [**1**][I] (4, 3.2 and 2.56 mM) for 2.5 h at 37 °C. Then the samples were loaded in 1% agarose gel in TAE buffer (pH = 8) at a current of 2 V cm^{-1} for 4 h.

Isothermal titration calorimetric (ITC) experiments

In a typical experiment, 7 μL aliquots of a 300 μM DNA solution were injected from a 250 μL rotating syringe (290 rpm) into the isothermal sample chamber containing 1.4235 mL [**1**][$CuCl_2$] solution (5 μM). Corresponding control experiments to determine the heat of dilution of DNA to the buffer were performed. Before use, all the solutions were degassed under vacuum (140 mbar, 8 min) on the thermovac to eliminate air bubble formation during titration. The duration of each injection was 10 s and the delay time between each injection was 300 s. The initial delay before the first injection was 60 s. Each injection generated a heat burst curve (micro calories per second *vs.* time). The area under each peak was determined by integration using the Origin software to give a measurement of the heat associated with the injection. The heat associated with each DNA–buffer titration was subtracted from the corresponding heat associated with each DNA–$[\mathbf{1}]^+$ injection to give the heat of binding for that injection.

UV optical melting study

In a typical experiment, the DNA was mixed with varying concentrations of [**1**][$CuCl_2$] in degassed buffer in micro-optical cuvettes of 1 cm path length and the temperature of the cuvette accessory was raised at a heating rate of 0.5 °C min^{-1}, in the range 20–110 °C, continuously monitoring the absorbance change at 260 nm. Melting curves allowed an estimation of the melting temperature T_m, the midpoint temperature of the [**1**][$CuCl_2$] bound CT-DNA unfolding process obtained from the maxima of the first derivative plots. The T_m value is reproducible to within ± 1 °C.

Results and discussion

Syntheses and characterization

The dark coloured crystalline parent compound [**1**][$CuCl_2$] was isolated in good yield from a reaction of phenanthrene-9,10-dione, *N*-phenylbenzene-1,2-diamine and anhydrous $CuCl_2$ in the presence of a catalytic amount of concentrated HCl in methanol (Scheme 1). In this reaction, cupric ions act as an oxidising agent and are themselves reduced to $[CuCl_2]^-$. [**1**][I] was synthesized by reacting [**1**][$CuCl_2$] with excess KI in methanol solution. The molecular compositions of [**1**][$CuCl_2$] and [**1**][I] were confirmed by elemental (C, H and N) analyses and ESI (+ve) mass spectra. IR spectra have confirmed the absence of NH bonds in [**1**][$CuCl_2$] and [**1**][I].

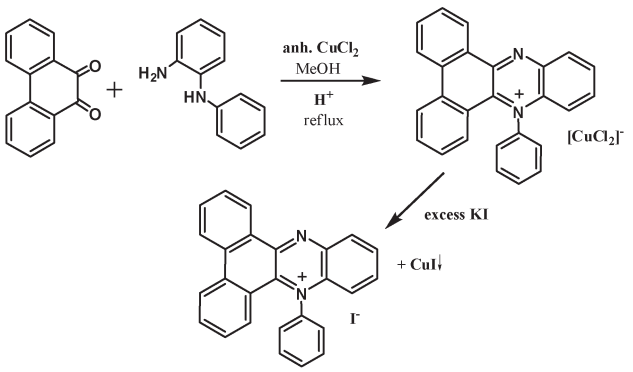

Scheme 1 Syntheses of [**1**][$CuCl_2$] and [**1**][I]

The UV-vis absorption spectral features of [**1**][$CuCl_2$] and [**1**][I] in dichloromethane are similar, as shown in Fig. 2. The absorption data are summarized in Table 2. Both [**1**][$CuCl_2$] and [**1**][I] are non-luminescent in solid or in solution.

Molecular structure of [1][$CuCl_2$]

Single crystal X-ray structure determination of [**1**][$CuCl_2$] has confirmed the molecular geometry of [**1**][$CuCl_2$] in crystals. [**1**][$CuCl_2$] crystallizes in the $P2_1/n$ space group. The molecular geometry is illustrated in Fig. 3 and selected bond parameters are listed in Table 3. The phenanthrene fragment including the condensed *N*-phenylbenzene-1,2-diamine unit makes a plane with a mean of 0.2 Å. The pendant phenyl ring is at 71° with the mean plane of the cation. The $CuCl_2^-$ anion is linear. The two Cu–Cl bond distances are approximately the same (Table 3) and are consistent with the Cu^I–Cl lengths reported in other copper(I) species.[11]

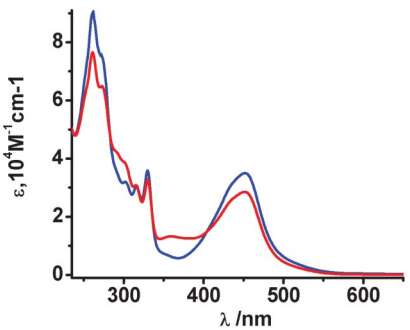

Fig. 2 Electronic spectra of [**1**][$CuCl_2$] (blue) and [**1**][I] (red) in CH_2Cl_2 at 25 °C.

Table 2 Electronic spectral data of [**1**][$CuCl_2$] and [**1**][I] in CH_2Cl_2 at 25 °C

Compound	λ_{max}/nm ($\varepsilon/10^5$ M^{-1} cm^{-1})
[**1**][$CuCl_2$]	452(3.54), 330(3.58), 316(3.06), 303(3.17), 273(7.53), 261(9.04)
[**1**][I]	452(2.88), 330(3.26), 316(3.07), 301(3.84), 273(6.49), 261(7.64)

DNA intercalation and spectral features

UV-vis spectra

A series of experiments were performed to determine the propensity of this compound to bind to DNA. The cationic [**1**][$CuCl_2$] complex has an absorption maximum around 440 nm that is convenient to monitor the interaction with DNA. Addition of DNA to the cation resulted in hypochromatic and bathochromic effects, indicating a strong intermolecular association (Fig. 1) involving the π electron cloud of the interacting cation and the base pair of DNA, presumably due to intercalation. The presence of a distinct isosbestic point at 465 nm suggests that two states, the bound and free form of the cationic species, occur in the reaction mixture at any wavelength. The λ_{max} of free and CT-DNA bound [**1**][$CuCl_2$] were 440 and 445 nm, respectively, while its λ_{iso} is at 465 nm, ε_f = 21,380 M^{-1} cm^{-1} (at 440 nm), ε_B = 14,407 M^{-1} cm^{-1} (at 440 nm), ε_{iso} = 74,250 M^{-1} cm^{-1} (at 465 nm) *etc.* Titration of a constant concentration of [**1**][$CuCl_2$] with DNA using several inputs of DNA was carried out and the data were utilized to construct a Scatchard plot of r/C_f *vs.* r, where r is the number of moles of the [**1**][$CuCl_2$] complex per mole base pairs. The Scatchard plot, depicted in the inset of Fig. 1, clearly reveals that at low values of r there is a negative slope, indicating non-cooperative binding. This enables fitting of the curves to a theoretical curve drawn according to the excluded site model of McGhee and von Hippel[8] for a non-cooperative binding system to derive the best-fit parameters of the intrinsic binding constant (K_i = 1.01 ± 0.1 × 10^5 M^{-1}) to an isolated binding site and the number of base pairs (n = 8) excluded by the binding of a single [**1**][$CuCl_2$] complex.

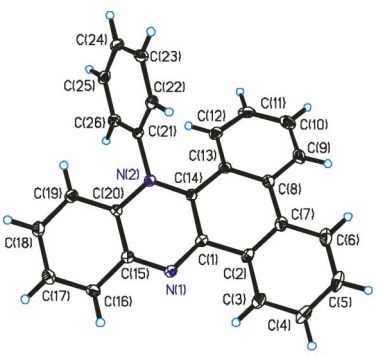

Fig. 3 An ORTEP plot of [**1**]$^+$ in the crystals of [**1**][$CuCl_2$] (linear $CuCl_2^-$ is omitted for clarity).

Table 3 Selected bond lengths (Å) of [**1**][$CuCl_2$]

Cu1–Cl1	2.106(6)	C14–N2	1.358(2)
Cu1–Cl2	2.110(6)	C1–C14	1.434(3)
C1–N1	1.326(2)	C1–C2	1.461(3)
C15–N1	1.350(2)	C15–C20	1.409(3)
C20–N2	1.385(2)	C13–C14	1.472(2)

Fluorescence spectra

To further substantiate the presumably intercalative DNA binding mode of the [**1**][$CuCl_2$] complex we studied its ability to displace DNA bound ethidium bromide.[12] The relative fluorescence intensity decrease of the CT-DNA–ethidium bromide complex of upon addition of [**1**][$CuCl_2$] is shown in Fig. 4. The results showed clearly that with an increase of the added concentration of [**1**][$CuCl_2$] the fluorescence intensity decreased steadily. Thus, the cationic [**1**][$CuCl_2$] complex is a very effective intercalator of DNA.

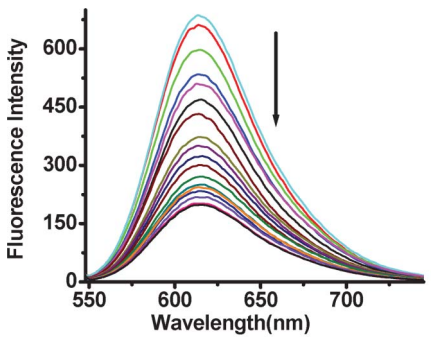

Fig. 4 Fluorescence titration data on the displacement of CT-DNA bound ethidium bromide by [**1**][$CuCl_2$].

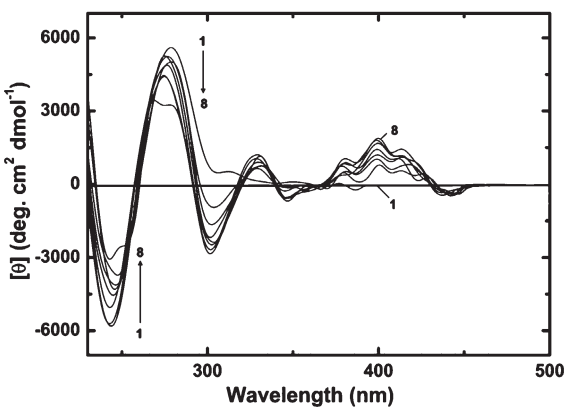

Fig. 5 CD spectra resulting from the interaction of [**1**][$CuCl_2$] with CT-DNA. Curves 1⟶8 denote the interaction of CT-DNA (60 μM) treated with 0, 3.2, 6.3, 8.5, 12.5, 18.3, 25.0 and 30.2 μM [**1**][$CuCl_2$].

CD spectra

[**1**][$CuCl_2$] is an optically inactive molecule and hence we used circular dichroism to further understand the interaction phenomenon. The CD spectrum of CT-DNA showed characteristic positive and negative bands around 270–280 and 243 nm, respectively, of the B-form structure, as given in Fig. 5. These CD bands of the DNA are caused due to stacking interactions between the bases and the helical structure, which provide an asymmetric environment for the bases.[13] Both the bands were perturbed in the presence of increasing concentrations of [**1**][$CuCl_2$], resulting in a decrease of the 275 nm band elipticity with a small blue shift and a concomitant decrease of the 248 nm band intensity. Changes in the CD spectra of the DNA on binding reflect an effective coupling of the transition moments of the bound [**1**][$CuCl_2$] with that of the base pairs and resulting from the intercalative binding record the [**1**][$CuCl_2$] induced changes in the CT-DNA conformation, the CD spectral changes on addition of various amounts of [**1**][$CuCl_2$], resulting in an increasing D/P ratio, were recorded in the region 210–400 nm. The observed decrease in the positive dichromic signal of DNA may be due to a transition from the extended nucleic acid double helix to the more compact form.[13]

The binding also induced optical activity in the $[\mathbf{1}]^+$ cations, as manifested by an induced CD spectrum resulting from the asymmetric environment of duplex DNA. The induced CD showed a negative maximum at 293 nm and a positive one in the range 252–286 nm with a peak at 278 nm. This may be due to an excitation splitting mechanism arising out of effective transition moments of the intercalation of $[\mathbf{1}]^+$ with base pairs of DNA. The increase in concentration of the cation $[\mathbf{1}]^+$ resulted in D/P value enhancement, the molar elipticity was lowered on either side of the nucleic acid absorption maximum and the magnitude of the induced CD spectra was higher and higher. This is clearly indicative of the more penetrative nature of the intercalator [**1**][$CuCl_2$].

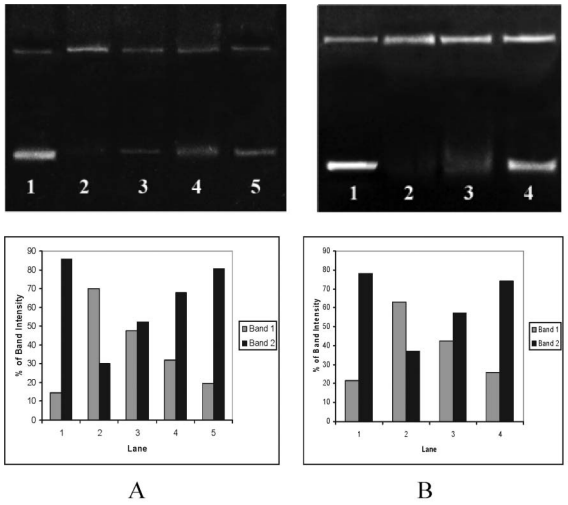

Fig. 6 Changes in the agarose gel electrophoretic pattern of pUC19 DNA induced by the $[\mathbf{1}]^+$ cation complexes [**1**][$CuCl_2$] and [**1**][I] (the upper panel indicates the band positions, while the lower panel shows band intensity). Lane 1 in the upper panel of both figures contains control pUC19 DNA; lanes 2, 3, 4 and 5 of panel A: [**1**][$CuCl_2$], 2.56, 1.92, 1.28 and 0.64 mM respectively. Lane 2, 3 and 4 of panel B: [**1**][I], 4, 3.2 and 2.56 mM respectively.

Gel-electrophoresis studies

The result of gel electrophoresis on the interaction of DNA (pUC 19) with [**1**][$CuCl_2$] and [**1**][I] complexes are shown in Fig. 6. Lane 1 of Fig. 6A and 6B highlights two bands of pUC19 DNA [upper band – nicked circular (NC), lower band – supercoiled (SC)]. Comparison of the DNA band intensity and position after making a complex with the cation $[\mathbf{1}]^+$ containing complex clearly shows an interaction of the cationic complex with DNA. Binding to DNA resulted in a change in the band density with respect to the highlighted bands for pUC19 as a control, shown in lane 1 of both Fig. 6A and 6B. It is evident from the figure that the interaction of higher concentrations of cation $[\mathbf{1}]^+$ resulted in shifting from SC to NC. In the case of the NC state there is a nick and that leads to linearization of the DNA molecule and hence the band position is retarded due to the size increase. It is clearly shown that the compounds [**1**][$CuCl_2$] and [**1**][I] are strong intercalators, which is supported by the CD spectral change after DNA binding with the compound (Fig. 5). In the case of [**1**][I], a concentration higher than that of [**1**][$CuCl_2$] was necessary to bring a similar change in the band pattern of DNA; this was possibly due to the lower solubility of the former complex. The overall pattern of the change in DNA band shift apparently suggests that the interaction is due to the cationic species of the complexes. If we compare the concentration of the complexes [**1**][$CuCl_2$] and [**1**][I] in lane 2 of Fig. 6A and lane 4 of Fig. 6B they are the same, but due to the much lower solubility of the iodide complex the effective concentration of cation $[\mathbf{1}]^+$ is much lower in the case of [**1**][I], hence the band intensity change is not identical.

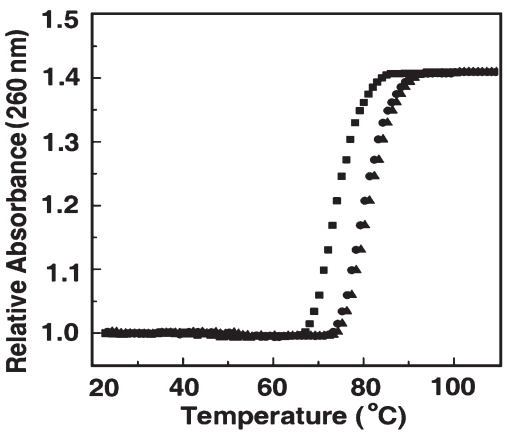

Fig. 7 Thermal melting profiles of CT-DNA (40 μM) (■) treated with [**1**][$CuCl_2$] at a drug–base pair molar ratio of 0.35 (●) and 0.65 (▲).

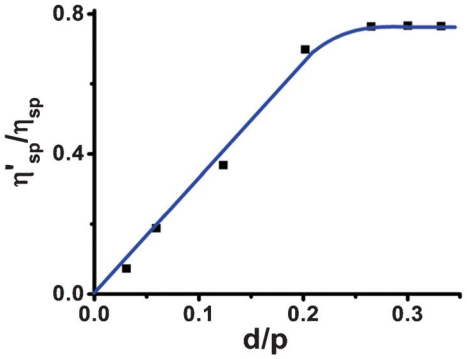

Fig. 8 Plot of change in relative viscosity of CT-DNA with increasing concentrations of [**1**][$CuCl_2$].

Optical melting and hydrodynamic studies

The binding of [**1**][$CuCl_2$] to the DNA was also evaluated from optical thermal melting studies.[7b] Double stranded calf thymus DNA under the conditions of the experiment melted with a T_m value of 75 °C (Fig. 7). The melting temperature of the DNA was enhanced on binding of [**1**][$CuCl_2$], and at saturation, a ΔT_m of about 7 °C was observed. Such a large stabilization of the DNA helix appears to be due to the strong binding of [**1**][$CuCl_2$] to the duplex DNA.

To confirm intercalation, we also exploited the changes in length and stiffening of the rod like structure of DNA, which is a diagnostic test in establishing the binding mode to DNA.[10,14] The hydrodynamic behaviour of the DNA as measured by the viscosity change of the complex is explored for this purpose. The results of viscosity increase with increasing doses of the [**1**][$CuCl_2$] complex are given in Fig. 8 and they clearly demonstrate that there is a sharp rise in viscosity, which attained a plateau indicating a maximum enhancement of the frictional resistance or change in the shape of CT-DNA on binding due to the intercalation of the [**1**][$CuCl_2$] complex between the base pairs of DNA.

Thermodynamic characterization

Finally, thermodynamical characterization of the DNA binding of [**1**][$CuCl_2$] was performed by highly sensitive isothermal titration calorimetry. ITC is a technique that can provide detailed information about the Gibbs energy, enthalpy of binding, the entropy contribution along with the binding constant and stoichiometry.[15] Fig. 9A shows the representative raw heat profile resulting from a typical ITC experiment in which DNA was titrated from the syringe into the [**1**][$CuCl_2$] solution in the calorimetric cell. The titration resulted in a single exothermic binding event, enabling the data to be fitted to a single set of identical binding sites model (Fig. 9B).

To extract the binding and thermodynamic parameters of the interaction, the thermogram was fitted to a single site model and the thermodynamic parameters were estimated

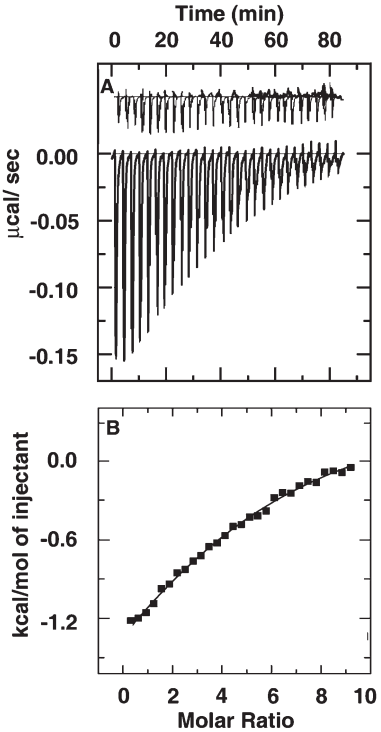

Fig. 9 ITC profile for the titration of CT-DNA into a solution of [**1**][$CuCl_2$] in phosphate buffer, pH 7.0 at 20 °C. Each heat burst curve in panel (**A**) is the result of a 7 μL injection from a 300 μM solution of DNA into the solution of [**1**][$CuCl_2$] (5 μM). The upper panel shows the heat burst for the injection of DNA into the same buffer as the control (curves offset for clarity). Panel (**B**) represents the corresponding normalized heat signals *versus* the molar ratio. The data points reflect the experimental injection heat while the solid line represents the calculated fit of the data.

from the best fit to the observed heat release. The data were analyzed with several different initial guesses and the resulting fits gave consistent values of the parameters, $K_a = 2.08 \pm 0.26 \times 10^5\ M^{-1}$, $\Delta H^0 = -14.05 \pm 1.40$ kcal mol^{-1}, a $T\Delta S^0$ of 0.162 kcal mol^{-1} and a binding site size of ~5 base pairs. The binding affinity obtained from ITC was in reasonable agreement with that obtained from the McGhee–von Hippel analysis of the absorbance data. The binding Gibbs energy change (ΔG^0) was −7.175 kcal mol^{-1}. The small entropy term suggested the binding of [**1**][$CuCl_2$] to CT-DNA to be predominantly enthalpically driven. The nucleic acid binding of several intercalators and groove binders has been shown to be very largely enthalpically driven.[16] It is likely that the intercalation of [**1**][$CuCl_2$] may involve a variety of non-covalent interactions including the strong stacking interactions from intercalation binding, all of which may contribute to the large negative enthalpy.

Conclusions

In summary, we present the syntheses and strong intercalative DNA binding properties of the novel 9-phenyldibenzo [*a*,*c*]phe-

nazin-9-ium $[1]^+$ cation and its complex. The structural data that proved the intercalative binding has been complemented with a gel electrophoresis pattern and energetics of the binding process, which was exothermically and enthalpically driven. The findings point to its potential usefulness as a DNA targeted therapeutic agent.

Acknowledgements

Financial support received from DBT, New Delhi, India (No. BT/PR13754/Med/29/181/2010) is gratefully acknowledged. SK and MKB are thankful to CSIR, New Delhi, India, for fellowships. KB was supported by the CSIR Research Associateship and AB was an INSPIRE fellow, DST. We are thankful to technical assistant Mr. Arpan Dey of VJRC R&D Center, Vijaygarh Jyotish Ray College, Kolkata.

Notes and references

1 (*a*) H.-K Liu and P. J. Sadler, *Acc. Chem. Res.*, 2011, **44**, 349; (*b*) N. J. Farrer and P. J. Sadler, *Aust. J. Chem.*, 2008, **61**(9), 669; (*c*) P. C. A. Bruijnincx and P. J. Sadler, *Curr. Opin. Chem. Biol.*, 2008, **12**, 197; (*d*) Y. Jung and S. J. Lippard, *Chem. Rev.*, 2007, **107**, 1387; (*e*) D. Wang and S. J. Lippard, *Nat. Rev. Drug Discovery*, 2005, **4**, 307; (*f*) H. Han and L. H. Hurley, *Trends Pharmacol. Sci.*, 2000, **21**, 136.

2 (*a*) K. Bhadra and G. S. Kumar, *Biochim. Biophys. Acta, Gen. Subj.*, 2011, **1810**, 485; (*b*) S. Nafisi, M. A. Khalilzadeh and Z. Mokhtari, *DNA Cell Biol.*, 2010, **29**, 753; (*c*) S. Nafisi, M. Bonsai, P. Maali, F. Manouchehri and M. A. Khalilzadeh, *J. Photochem. Photobiol., B*, 2010, **100**, 84; (*d*) C. D. Kanakis, S. Nafisi, A. Shadaloi, M. Rajabi and H. A. Tajmir-Riahi, *Spectroscopy Biomedical Applications*, 2009, **23**, 29; (*e*) S. Nafisi, F. Manouchehri and H. A. Tajmir-Riahi, *J. Mol. Struct.*, 2008, **875**, 392; (*f*) M. Maiti and G. S. Kumar, *Med. Res. Rev.*, 2007, **27**, 649; (*g*) S. Nafisi, F. Ghoreishi and H. A. Tajmir-Riahi, *J. Mol. Struct.*, 2007, **830**, 182; (*h*) S. Nafisi, A. A. Saboury, N. Keramat and H. A. Tajmir-Riahi, *J. Mol. Struct.*, 2007, **827**, 35; (*i*) R. Martínez and L. Chacón-García, *Curr. Med. Chem.*, 2005, **12**, 127; (*j*) M. S. Butler, *J. Nat. Prod.*, 2004, **67**, 2141; (*k*) G. Bischoff, S. Hoffmann, R. Martínez and L. Chacón-García, *Curr. Med. Chem.*, 2002, **9**, 321; (*l*) L. H. Hurley, DNA and its associated processes as targets for cancer therapy, *Nat. Rev. Cancer 2.*, **2002**, 188; (*m*) L. H. Hurley, *Biochem. Soc. Trans.*, 2001, **29**, 692; (*n*) D. E. Graves and L. M. Velea, *Curr. Org. Chem.*, 2000, **4**, 915; (*o*) M. J. Martinez, DNA modification and cancer, *Annu. Rev. Bichem.*, 1981, **50**, 159; (*p*) M. J. Martinez, *Annu. Rev. Biochem.*, 1981, **50**, 159.

3 (*a*) S. Dhar, N. Kolishetti, S. J. Lippard and O. C. Farokhzad, *Proc. Natl. Acad. Sci. U. S. A.*, 2011, **108**, 1850; (*b*) S. Tabassum and I. H. Bhat, *Chem. Pharm. Bull.*, 2010, **58**(3), 318; (*c*) R. C. Todd and S. J. Lippard, *J. Inorg. Biochem.*, 2010, **104**, 902; (*d*) S. Roy, S. Saha, R. Majumdar, R. R. Dighe and A. R. Chakravarty, *Polyhedron*, 2010, **29**, 2787; (*e*) D. Lahiri, R. Majumdar, A. K. Patra and A. R. Chakravarty, *J. Chem. Sci.*, 2010, **122**, 321; (*f*) B. Maity, M. Roy, B. Banik, R. Majumdar, R. R. Dighe and A. R. Chakravarty, *Organometallics*, 2010, **29**, 3632; (*g*) O. Novakova, J. Malina, T. Suchankova, J. Kasparkova, T. Bugarcic, P. J. Sadler and V. Brabec, *Chem. A Eur. J.*, 2010, **16**, 5744; (*h*) Y. Fu, A. Habtemariam, A. M. Pizarro, S. H. van Rijt, D. J. Healey, P. A. Cooper, S. D. Shnyder, G. J. Clarkson and P. J. Sadler, *J. Med. Chem.*, 2010, **53**, 8192; (*i*) S. Tabassum and I. H. Bhat, *Spectrochim. Acta, Part A*, 2009, **72**, 1026; (*j*) S. Tabassum, I. H. Bhat and E. Arjmand, *Spectrochim. Acta, Part A*, 2009, **74**, 1154; (*k*) A. M. Pizarro and P. J. Sadler, *Biochimie*, 2009, **91**, 1198; (*l*) S. Tabassum and S. Mathur, *Chem. Biodiversity*, 2006, **3**, 312; (*m*) S. M. Cohen and S. J. Lippard, *Prog. Nucleic Acid Res. Mol. Biol.*, 2001, **67**, 93; (*n*) B. Lippert, in *Chemistry and Biochemistry of a Leading Anticancer Drug*, Wiley-VCH, Weinheim, Germany, 1999.

4 (*a*) P. Paul, M. Hossain, R. C. Yadav and G. S. Kumar, *Biophys. Chem.*, 2010, **148**, 93; (*b*) K. Gurova, *Future Oncol.*, 2009, **5**, 1685.

5 (*a*) M. Sinan, M. Panda, A. Ghosh, K. Dhara, P. E. Fanwick, D. J. Chattopadhyay and S. Goswami, *J. Am. Chem. Soc.*, 2008, **130**, 5185; (*b*) D. E. Graves and L. M. Velea, *Curr. Org. Chem.*, 2000, **4**, 915; (*c*) G. S. Kumar, Q. Y. He, D. Behr-Ventura and M. Tomasz, *Biochemistry*, 1995, **34**, 2662.

6 (*a*) G. M. Sheldrick, *ShelXS97*, Universität Göttingen: Göttingen, Germany, 1997; (*b*) G. M. Sheldrick, *ShelXL97*, Universität Göttingen: Göttingen, Germany, 1997.

7 (*a*) R. Sinha and G. S. Kumar, *J. Phys. Chem. B*, 2009, **113**, 13410; (*b*) K. Bhadra, M. Maiti and G. S. Kumar, *Biochim. Biophys. Acta, Gen. Subj.*, 2007, **1770**, 1071; (*c*) J. B. Chaires, N. Dattagupta and D. M. Crothers, *Biochemistry*, 1982, **21**, 3933.

8 J. D. McGhee and P. H. von Hippel, *J. Mol. Biol.*, 1974, **86**, 469.

9 (*a*) R. Sinha, M. Hossain and G. S. Kumar, *Biochim. Biophys. Acta, Gen. Subj.*, 2007, **1770**, 1636; (*b*) A. Ray, M. Maiti and A. Nandy, *Comput. Biol. Med.*, 1996, **26**, 497.

10 (*a*) S. Satyanarayana, J. C. Dabrowiak and J. B. Chaires, *Biochemistry*, 1992, **31**, 9319; (*b*) M. Maiti, R. Nandi and K. Chaudhuri, *FEBS Lett.*, 1982, **142**, 280.

11 (*a*) M. Hargittai, P. Schwerdtfeger, R. Balázs and R. Brown, *Chem.–Eur. J.*, 2003, **9**, 327; (*b*) L. Bernasconi, E. Fois and A. Selloni, *J. Chem. Phys.*, 1999, **110**, 9048; (*c*) S. Ves, D. Glötzel, M. Cardona and H. Overhof, *Phys. Rev. B*, 1981, **24**, 3073.

12 (*a*) M. Lee, A. L. Rhodes, M. D. Wyattt, S. Forrow and J. A. Hartley, *J. Med. Chem.*, 1993, **36**, 863; (*b*) M. Lee, A. L. Rhodes, M. D. Wyattt, S. Forrow and J. A. Hartley, *Anti cancer Drug Des.*, 1993, **8**, 173.

13 A. Rajendran and B. U. Nair, *Biochim. Biophys. Acta, Gen. Subj.*, 2006, **1760**, 1794.

14 R. Sinha, M. M. Islam, K. Bhadra, G. S. Kumar, A. Banerjee and M. Maiti, *Bioorg. Med. Chem.*, 2006, **14**, 800.

15 (*a*) K. Bhadra and G. S. Kumar, *Mini-Rev. Med. Chem.*, 2010, **10**, 1235; (*b*) N. J. Buurma and I. Haq, *Methods*, 2007, **42**, 162; (*c*) A. L. Faig, *Biopolymers*, 2007, **87**, 293.

16 (*a*) S. R. Chowdhury, M. M. Islam and G. S. Kumar, *Mol. BioSyst.*, 2010, **6**, 1265; (*b*) A. Adhikari, M. Hossain, M. Maiti and G. S. Kumar, *J. Mol. Struct.*, 2008, **889**, 54; (*c*) J. B. Chaires, *Arch. Biochem. Biophys.*, 2006, **453**, 26; (*d*) J. Ren, T. C. Jenkins and J. B. Chaires, *Biochemistry*, 2000, **39**, 8439; (*e*) A. Das and G. S. Kumar, *J. Chem. Thermodyn.*, 2012, **54**, 421.